Closer look into the structures of tetrabutylammonium bromide–glycerol-based deep eutectic solvents and their mixtures with water

Patrycja Makoś-Chełstowska [a*], Renáta Chromá [b], Vasil Andruch [b]

[a] *Department of Process Engineering and Chemical Technology, Faculty of Chemistry, Gdansk University of Technology, Gdansk, PL-80-233 Gdańsk, Poland*

[b] *Department of Analytical Chemistry, Institute of Chemistry, Faculty of Science, Pavol Jozef Šafárik University in Košice, SK-04154 Košice, Slovakia*

*Corresponding author: dr Patrycja Makoś-Chełstowska, PhD. Eng.,
e-mail: patrycja.makos@pg.edu.pl

Abstract: In recent years, deep eutectic solvents (DES) and it's mixture with water have become more and more attention as green solvents used in chemistry. However, there are only a few theoretical studies on the mechanisms of pure DES and DES-water complex formation. Therefore, the structural properties of tetrabutylammonium bromide–glycerol-based deep eutectic solvents and their mixtures with water have been investigated by means of Molecular Dynamics simulations. The obtained results indicate that three types of H-bonds exist in the pure DES structures, and all of these interactions play an important role in DES formation. In addition, between hydrogen bond donors (HBDs) and hydrogen bond acceptor (HBA) weaker non-bonded interactions, i.e. van der Waals exist, which also contribute to the formation of stable DES structures and to lower the melting point of DES compared to pure substances. The small addition of water to DES provides the formation of a stable complex, however, a further increase in water content (higher than 50% v/v) provide to the destruction of the most important hydrogen bonds (O–H···Br) in DES structure.

Keywords: Deep eutectic solvents, Tetrabutylammonium bromide, Glycerol, Theoretical calculations

Abbreviations

ATPB, Allyltriphenylphosphonium bromide;
BTPB, Benzyltriphenylphosphonium chloride;
ChCl, Choline chloride;
CAC, Choline acetyl chloride;
DAC, *N,N*-diethylethanolammonium chloride;
DES, Deep eutectic solvent;
EG, Ethylene glycol;
FT-IR, Fourier transform infrared spectroscopy;
Gly, Glycerol;
HBA, Hydrogen bond acceptor;
HBD, Hydrogen bond donor;
LA, Levulinic acid;
MTPB, Methyl triphenyl phosphonium bromide;
Pro, Propionic acid;
RDF, Radial distribution function;
RDG, Reduced density gradient
TBAB, Tetrabutylammonium bromide;
TBAC, Tetrabutylammonium chloride;
TBPB, Tetrabutylphosphonium bromide;
TEAC, Tetraethylammonium chloride.

1. Introduction

Deep eutectic solvents (DES) were designed more than a decade ago as a possible alternative to ionic liquids [1]. DESs are a combination of various hydrogen bond acceptors (HBAs) and hydrogen bond donors (HBDs). Thanks to some of their unique properties, they have been utilized in various fields of science and technology. TBAB-based and Gly-based DESs have been applied for a variety of purposes, selected examples of which are presented below.

The reversible absorption of SO_2 in six DESs composed of levulinic acid (LA) and various quaternary ammonium salts – ChCl, CAC, TEAC, TEAB, TBAC and TBAB – at a fixed 3:1 molar ratio was studied. All the examined DESs were capable of absorbing SO_2 and showed high selectivity for SO_2/CO_2. The effect of water content on SO_2 absorption was also investigated. The absorption capability of the LA–ChCl DES decreased slightly with increasing water content (5 and 10%), indicating a slight change in the structure and efficacy of the DES. The interaction of the LA–ChCl DES and SO_2 was examined by NMR and FT-IR spectroscopy, with the results showing the physical interaction between the DES and dissolved SO_2 [2]. The physicochemical properties of these DESs, such as density, dynamic viscosity, electrical conductivity and refractive index, were later investigated [3]. Wu et al. investigated the absorption capability of H_2S of two series of DESs based on TBAB or ChCl as the HBA with carboxylic acids (formic acid, acetic acid and propionic acid) as the HBD at various molar ratios. The solubility of H_2S increased with decreasing carboxylic acid concentration in the DES and was higher for TBAB-based DESs compared to ChCl-based ones, with TBAB:Pro showing the best results [4]. Hizaddin et al. [5]

investigated the extractive denitrogenation of diesel fuel using ammonium- and phosphonium-based DESs (TBAB and TBPB) and ethylene glycol at a 1:2 molar ratio. The DESs were tested to remove 5-membered nitrogen compounds (pyrrole and indoline) and 6-membered nitrogen compounds (pyridine and quinoline) from a model diesel compound (n-hexadecane). Phosphonium-based DESs show higher values of the distribution coefficient (D) and selectivity (S) than ammonium-based ones towards nitrogen compounds. Moreover, the investigated DESs have higher values of D and S towards 5-membered nitrogen compounds than for 6-membered ones [5]. Aqueous bi-phasic systems based on TBAB-based DESs were developed and applied in the rapid extraction of DNA from salmon testes. Four DESs based on TBAB and ethylene glycol, propylene glycol, butylene glycol and butyl alcohol were synthesized and tested. TBAB–EG and sodium sulfate were selected as the appropriate phase components. The interaction between DNA and the DES was confirmed by FT-IR spectra, circular dichroism spectra, dynamic light scattering and transmission electron microscope [6].

A few papers can be found devoted to the study of the physical properties of TBAB-Gly DESs. Yusof et al. studied the effect of HBD percentages, HBD type and temperature on the density, viscosity and ionic conductivity of DESs formed by TBAB with alcohol-based HBDs (ethylene glycol, 1,3-propanediol, 1,5-pentanediol and glycerol). DESs based on TBAB-glycerol had the highest density and viscosity and the lowest ionic conductivity when compared to other DESs, probably due to the extra hydroxyl group of glycerol [7]. The physical properties (freezing point, density, viscosity, conductivity, and surface tension) of six DESs based on glycerol as the HBD and six different salts (MTPB, BTPB, ATPB, ChCl, DAC, TBAB) at various molar ratios of the HBD to the salts were studied. Ammonium-based salt DESs had much lower viscosities than phosphonium-based salt DESs. Within the ammonium group, the viscosities of the different DESs increased as their molecular weights increased [8].

Besides the physicochemical properties of DESs, their formation mechanisms are quite significant for further application. It's well-known that hydrogen bonds between the HBA and the HBD play a dominant role in eutectic mixture formation. In order to identify H-bonds, spectroscopic methods, including FT-IR and NMR, are typically used [8,9]. As observed in other work, weaker non-bonded interactions can also determine DES formation [10]. In a previous work [11], we reported the NMR, IR and Raman spectra of a TBAB–Gly-based DES at various HBA:HBD molar ratios for neat DES as well as a DES with various amounts of water added. However, it is very difficult to identify these interactions through experimental methods [12–14]. For this purpose, a theoretical quantum mechanical calculation, which is a forceful tool for simulating molecular structures, can be used. However, only the combination of experimental and theoretical research enables complete insight into DES formation [15]. Therefore, herein we report the theoretical quantum mechanical calculations of tetrabutylammonium bromide–glycerol-based deep eutectic solvents and their mixtures with water. The simulations presented in the paper fully complement the previous experimental work [11].

2. Computational studies

The theoretical analysis of deep eutectic solvents composed of tetrabutylammonium bromide and glycerol in various molar ratios (1:2, 1:3, 1:4) and DES-water complexes were studied based on previous studies [10,16–20]. All the calculations, including molecular structure optimization and vibrational frequencies of the TBAB, Gly, water and DES, were performed based on the Beck3–Lee–Yang–Parr (B3LYP) level with the use of the 6-31+G** basis set. This basis set is large enough to calculate the vibrational frequencies and structure of deep eutectic solvents composed of TBAB and Gly in various molar ratios [21,22]. All the optimized configurations of deep eutectic solvents were tested to be local minima by frequency calculations. The interactions energy (ΔE) between the HBA and HBD in the DES molecule was calculated from equation (1):

$$\Delta E = E_{DES} - (E_{HBA} - E_{HBD}) \tag{1}$$

Where: E_{DES} is the total energy of DES composed of the HBA and HBD [kcal/mol], and E_{HBA}, and E_{HBD} are the individual energies of the HBA and HBD, respectively [kcal/mol].

The interactions energy between the DES composed of TBAB and Gly in a 1:3 molar ratio and water was calculated according to the equation (2):

$$\Delta E = E_{DES-H2O} - (E_{DES} - E_{H2O}) \tag{2}$$

where: $E_{DES\text{-}H2O}$ is the total energy of the complex composed of the DES and water [kcal/mol], and E_{DES} and E_{H2O} are the individual energies of the DES and water [kcal/mol].

The counterpoise procedure was used to account for the basis set superposition error (BSSE) [23]. The structures and atom definitions of DESs are presented in the Figure 1.

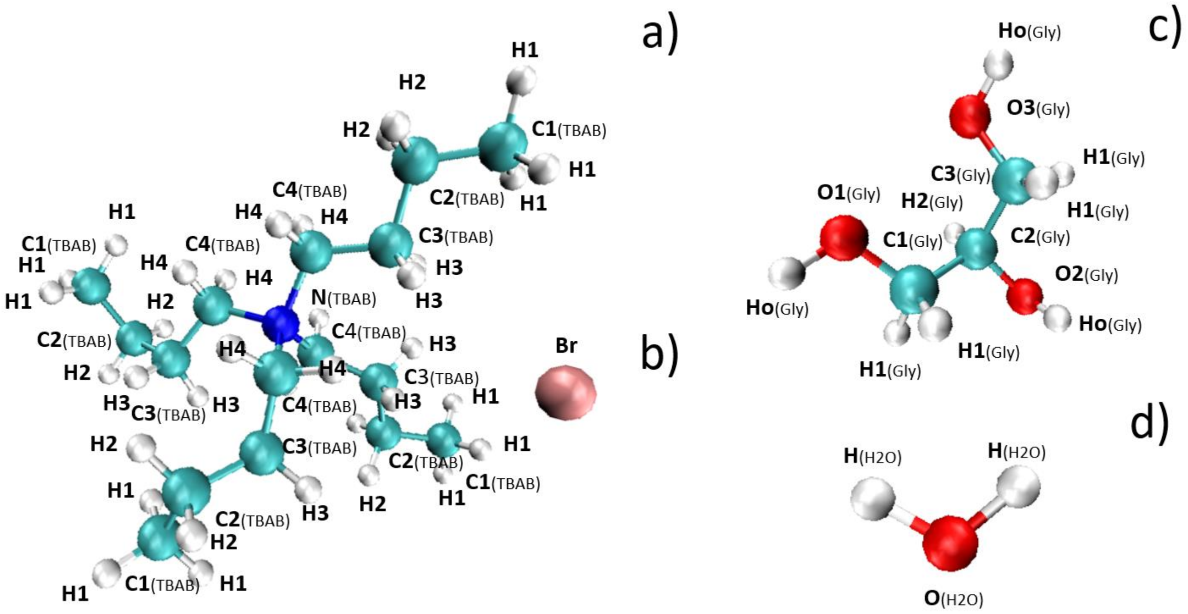

Figure 1 Geometries of a) tetrabutylammonium cation; b) bromide anion; c) glycerol; d) water.

For better discussion of the nature of the interactions between the HBA and HBD, as well as between the DES, a reduced density gradient (RDG) was applied. The RDG analysis was made using the Multiwfn software [24–26]. The Visual Molecular Dynamics 1.9.3. software was used to graphically present the results. In the further studies, for the pure DES in 1:2, 1:3, and 1:4 molar ratio, 100 TBAB and 200, 300, and 400 Gly molecules, were introduced onto a box, defined by the minimum coordinates x, y and z = 0. 0. 0. and maximum coordinates 40. 40. 40. The distance tolerance between atoms was 2.0 Å. In the next step, 100 TBAB:Gly (1:3) molecules and water molecules were placed in the box (Table 1), using PackMol code [27]. All computational studies were performed at constant pressure (1 bar) using Parrinello−Rahman barostat [28] and constant temperature (293.15 K) by means of Nose−Hoover thermostat [29,30] for the equilibration of all of the systems for 20−25 ns. In the simulations, a 10 ns production run was carried out with a trajectory saving frequency of 0.1 ps to compute structural properties of all studied systems. Force field parameters were derived from OPLS-AA model. In addition, the rigid SPC/E model was adopted for water molecules [31]. The presented simulations were performed by means of GROMACS 2020.5 software [32,33].

Table 1 Compositions of DES-H_2O complexes investigated in the present work

DES-H_2O complex	**Number of molecules**		
	TBAB	**Gly**	**H_2O**
TBAB:Gly (1:3)	100	300	0
80% TBAB:Gly (1:3)-20%H_2O	100	300	100
50% TBAB:Gly (1:3)-50%H_2O	100	300	200
20% TBAB:Gly (1:3)-80%H_2O	100	300	700
10% TBAB:Gly (1:3)-90%H_2O	100	300	2300

3. Results and Discussion

3.1. Deep eutectic solvents structures

Information of mechanism of DES (TBAB:Gly in 1:2, 1:3, 1:4 molar ratios) formation and influence of water addition on the DES structures which were obtained from the previous studies based on spectroscopic analysis i.e. Raman, FT-IR, ^{1}H NMR, ^{13}C NMR are not unambiguous, and they only indicate the existence of strong hydrogen bonds between the hydrogen bond donors and hydrogen bond acceptors [11]. However, they do not indicate the number of hydrogen bonds, their exact location and information on weaker interactions, i.e. the electrostatic interactions in the DES structures. Therefore, theoretical studies of were carried out to better understand the mechanism of DES formation.

The most stable and probable complexes in the gas phase of TBAB:Gly (1:2); TBAB:Gly (1:3); TBAB:Gly (1:4) were geometry optimized at the B3LYP/6-31+G** level of theory. The results of geometry optimization of the DES complex are presented in Figure 2. The geometric results show that in all DES configurations, nonbonded interaction exists between the Br atom from TBAB and Gly molecules, which can be identified as strong hydrogen bonds because of the short distances between the atoms (below 2.5 Å) [34]. In the TBAB:Gly (1:2) structure, the distances between the Br atom and the hydroxyl groups from the glycol O–H···Br are 2.23 Å and 2.41 Å. In TBAB:Gly (1:3) these distances are 2.27 Å, 2.29 Å and 2.47 Å and in TBAB:Gly (1:4) 2.64 Å, 2.40 Å, 2.62 Å and 1.86 Å. This indicates that with increasing glycerol content in the DES, the hydrogen bonds between the HBA and HBD weaken (O–H···Br). In addition, strong hydrogen bonds can be identified between the –OH groups in the glycerol molecules. The distances O–H···H–O are 1.93 Å in TBAB:Gly (1:2), 2.42 Å in TBAB:Gly (1:3) and 1.81 Å and 2.40 Å in TBAB:Gly (1:4). In all Gly molecules, intramolecular hydrogen bonds (O–H···H–O) occur for which the distances are in range from 1.81 to 2.23 Å. In all complexes the distance between the TBAB molecule and the Gly molecules is higher than 2.5 Å, which indicates that other weaker, non-covalent interactions exist.

Under real conditions, a DES composed of TBAB and Gly in a 1:2 molar ratio is solid at room temperature, which indicates that two H-bonds between the HBA and HBD is not enough for the formation of the eutectic mixture. TBAB:Gly (1:3) is a liquid with a tendency to crystallize after a few days. This shows that the three H-bonds between TBAB and Gly are a minimum for the formation of a liquid complex. On the other hand TBAB:Gly (1:4) is a liquid at room temperature and contains only two hydrogen bonds between the HBA and HBD, which indicates that the hydrogen bonds between the Gly molecules also play a main role in eutectic mixture formation.

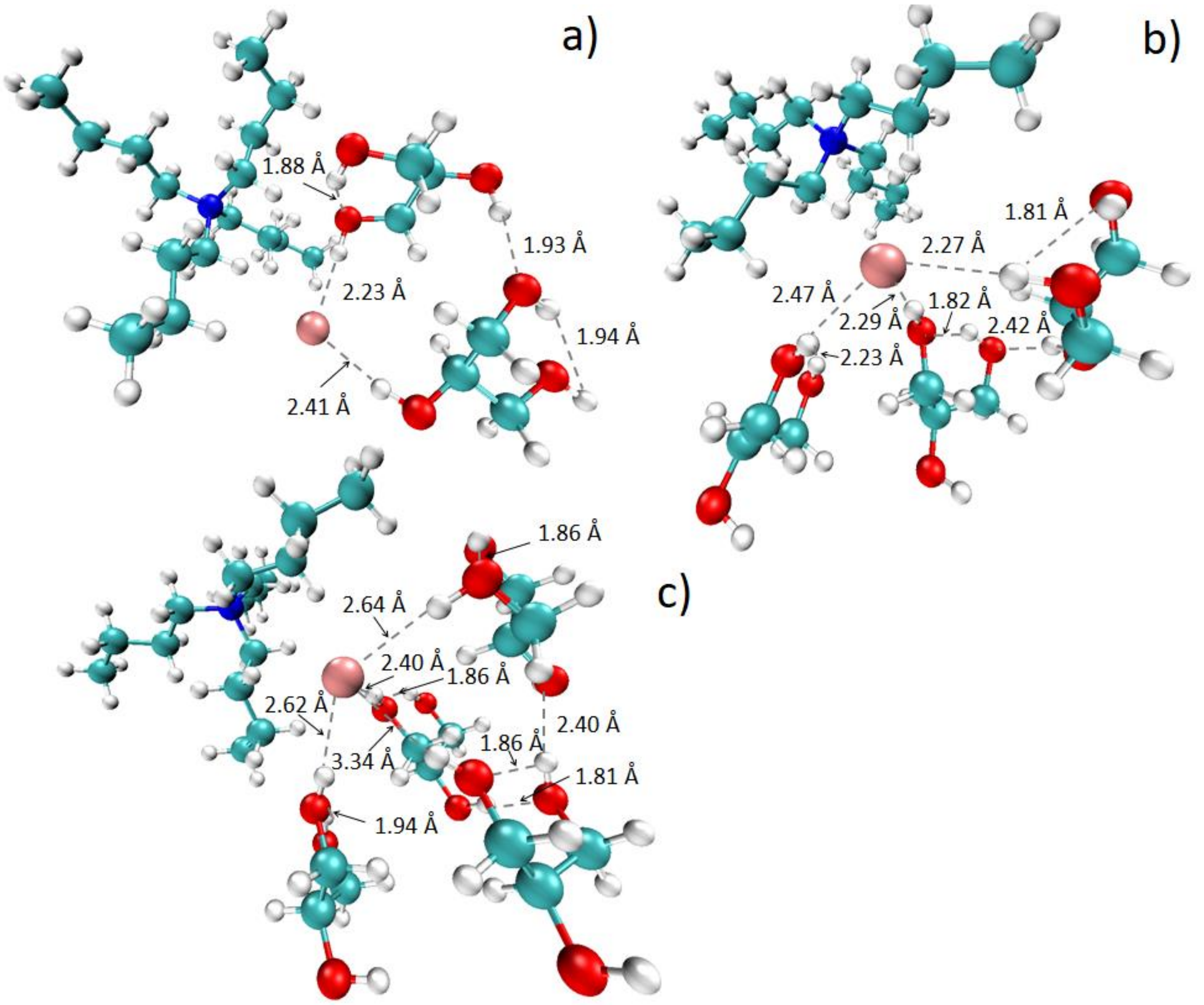

Figure 2 Optimized structures of a) TBAB:Gly (1:2); b) TBAB:Gly (1:3); TBAB:Gly (1:4).

To better describe the nature of the intermolecular interaction of the DESs and to confirm the existence of hydrogen bonds between the HBA and HBD, the reduced density gradient (RDG) method was employed. RDG is a useful method for detecting weak interactions based on electron density and its derivatives. It enables identification of both strong hydrogen bonds and van der Waals interactions, as well as steric repulsion in molecules [26]. A graphical interpretation of the obtained results is presented in Figure 3, where blue areas represent strong attractive effects (hydrogen bond); red areas indicate strong repulsive interactions; and green areas denote weaker noncovalent interactions, including van der Waals interaction. The obtained results show that in TBAB:Gly (1:2) two hydrogen bonds between the Br atom and the –OH groups from Gly, two intermolecular H-bonds in Gly molecules, as well as one hydrogen bond between the hydroxyl group from Gly existed, which correspond to the negative sign(λ2)ρ value (from –0.04 to –0.02 a.u.) in the 2D diagram (Figure 3). In addition, van der Waals interactions also occurred in the TBAB:Gly (1:2) complex between the HBA and HBD with 0.01 a.u. < sign(λ2)ρ < 0.01 a.u. values. The same interactions exist in TBAB:Gly (1:3) and TBAB:Gly (1:4). However, there are no additional hydrogen bonds, and only weaker van der Waals interactions exist between the third and fourth Gly molecule and the Br atom, as well as between the Gly molecules. The coexistence of both types of non-bonded interactions, i.e. hydrogen bonds and van der Waals interaction between TBAB and Gly molecules, corresponds to the formation of a stable deep eutectic solvent complex.

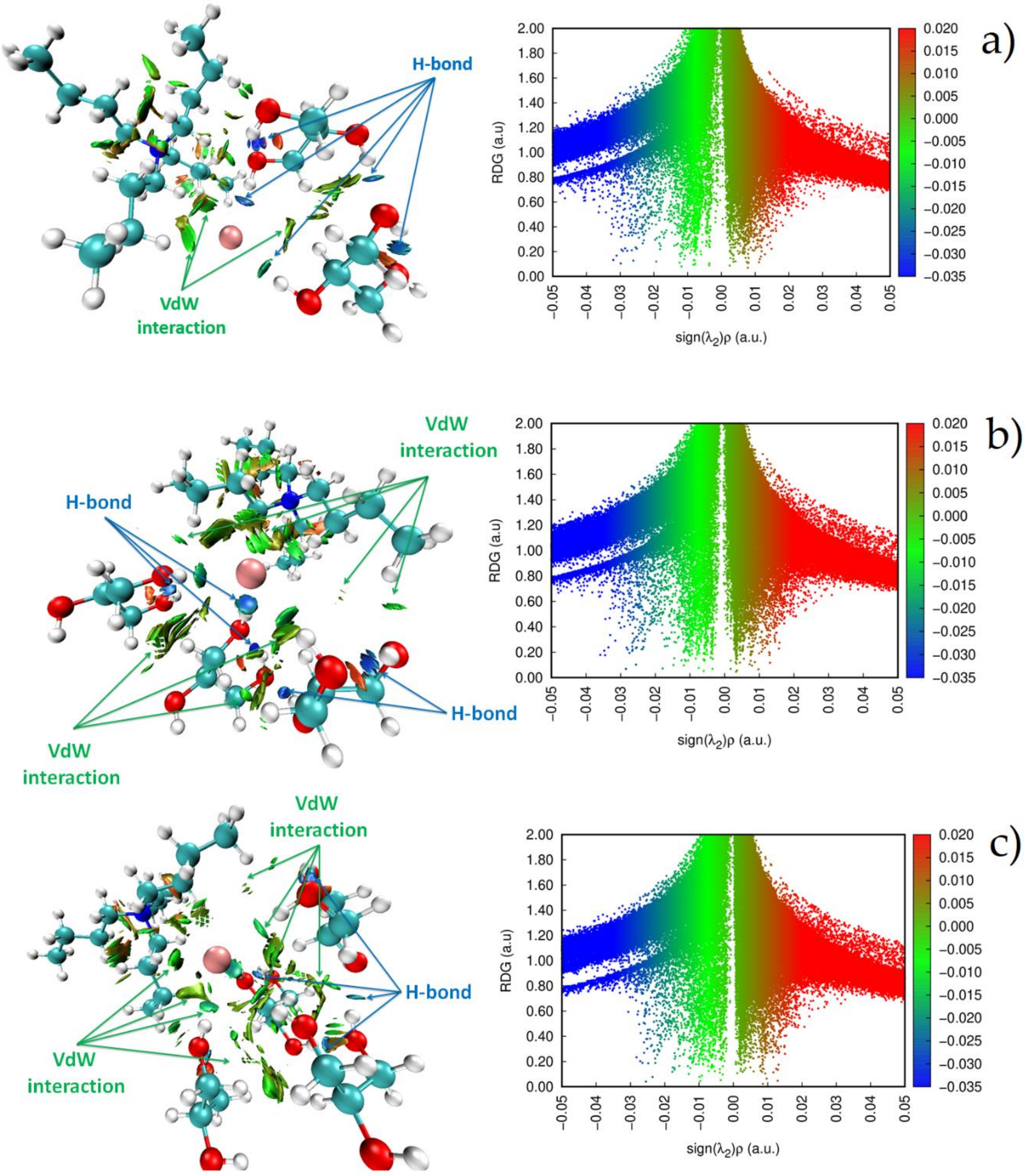

Figure 3 Reduced density gradient isosurfaces (s = 0.5 a.u.) and 2D diagrams of electron density and its reduced density gradient for a) TBAB:Gly (1:2); b) TBAB:Gly (1:3); c) TBAB:Gly (1:4).

In order to study the interactions between DES components in larger systems, the center of mass Radial distribution functions (RDF) were studied (Figure 4). The obtained results indicate that the increase in the numbers of Gly molecules in the DES-complexes practically does not weaken TBA^+–TBA^+ and TBA^+–Gly correlations, because the shifts and decrease first peaks intensity is not observed (Figure

4 a,e). An increase in the number of Gly in DES causes an increase in the intensity of the peaks and a shift of the peaks towards lower values in Gly–Gly and Br–Gly molecules. This indicates that additional hydrogen bonds are being formed between the glycols (Gly–Gly) within DES or between DES molecules (Figure 4b), as well as between Br– and Gly in DES structure (Figure 4f). However, in Br–Gly correlation the increase in peak intensity is observed after the addition of three Gly molecules, while after the addition of four Gly molecules to the DES structure, the intensity of peak does not change. This indicates that there are no additional strong interactions (i.e. hydrogen bonding) between Br and Gly after a further increase in numbers of Gly molecules. It can be assumed that further increasing the Gly in the DES structure would result in the formation of glycerol dimers. In contrast the inverse relationships can be observed for Br^-–Br^- and TBA^+–Br^- systems. This indicates that Br^-–Br^- and TBA^+–Br^- correlations become weaker and the nearest neighbor distance between ions increases with the increase of Gly molecules in DES systems. In all DES systems, correlation of Gly– Br^- is more prominent than TBA^+– Br^-, which indicate that the Gly–Br play an important role in DES formation, which was also observed in another DES complex [19,20,35].

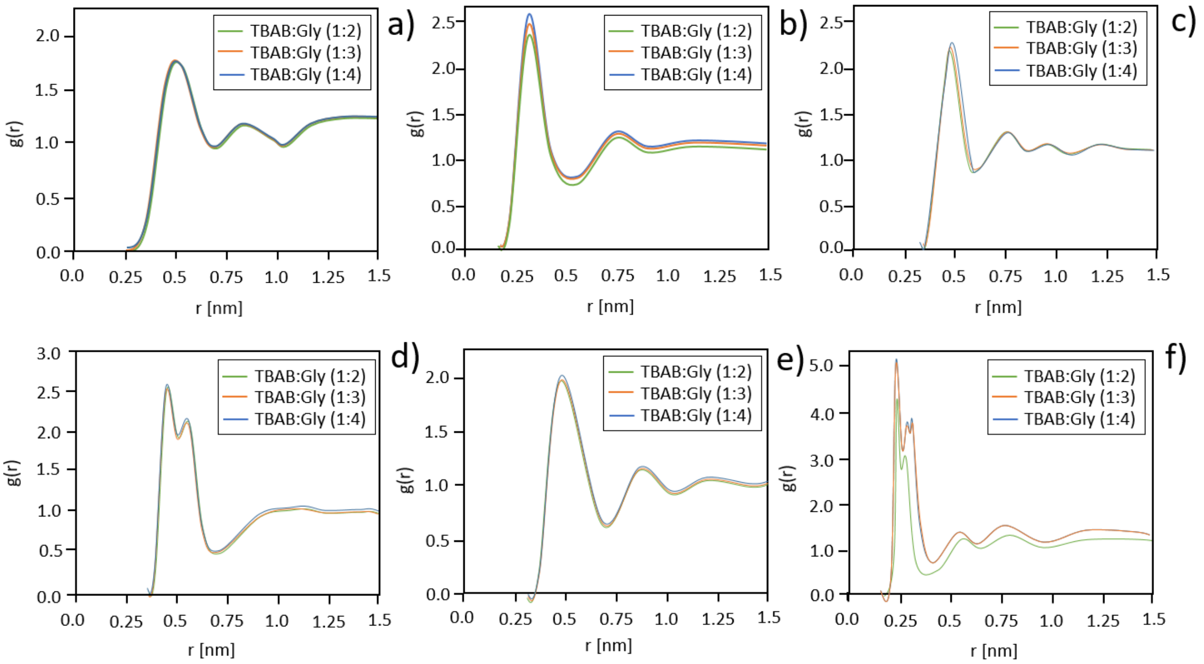

Figure 4 Intermolecular canter of mass Radial distribution functions (RDF) for a) TBA^+–TBA^+; b) Gly–Gly; c) Br^-–Br^-; d) TBA^+–Br^-; e) TBA^+–Gly; f) Br^-–Gly.

The atomic RDF enables the identification of hydrogen bonds between molecules in large DES systems. Based on the previous experimental studies [11] and geometric optimization of the simple single DES structures, it can conduct that in DES molecule, the three type of hydrogen bonds exist (between hydroxyl group from Gly and Br^-, between hydroxyl groups from Gly molecules (Gly–Gly) within DES, and intermolecular O–H···H–O in the Gly structure. However, in DES formation process only two types of H-bonding play dominant role ($Br\cdots HO_{(Gly)}$ and $OH_{(Gly)}\cdots HO_{(Gly)}$). Therefore, in further studies this two type of interactions were taken into a count. The results of atomic RDF indicate that the first peak in $Br\cdots HO_{(Gly)}$ correlation, slightly shifts towards a lower distance value in TBAB:Gly (1:3) relative to TBAB:Gly (1:2) (Figure 5). In addition, the increase of intensity of the first peak can be observed after an increase of Gly content in the DES structures. However, further addition of Gly molecules in the DES structure does not provide any change in the atomic RDF chart. The peaks in both systems almost overlap. This indicates that despite the addition of an additional Gly molecule, no additional hydrogen bonds are formed between $OH_{(Gly)}$–Br. On the other hand, shifts of the first peak towards lower values and an increase in peak intensity after increasing the Gly content in the DES structure, indicate the formation of hydrogen bonds between glycol molecules. This probably leads to the formation of Gly dimers.

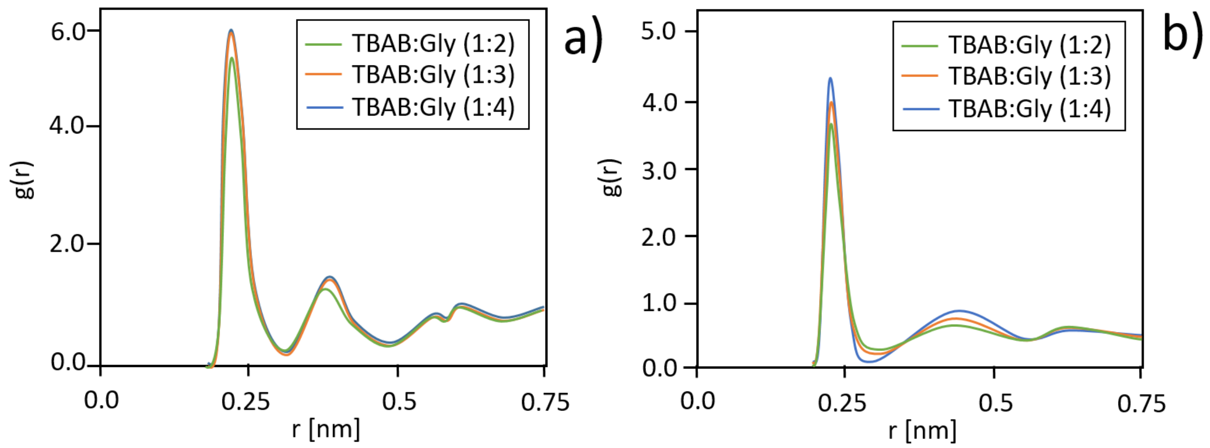

Figure 5 Atomic Radial distribution functions (RDF) for a) Br^{-}–$HO_{(Gly)}$, b) $HO_{(Gly)}$–$HO_{(Gly)}$.

3.2. Mixtures of deep eutectic solvents and water

In the next part of studies, simple single molecule system TBAB:Gly (1:3) with the addition of one, two, seven and twenty-three water molecules which represent the DES:H2O 20:80%, 50:50%; 80:20% and 90:10% volumetric ratio, were analyzed. The experimental density values at 20°C are 1.145, and 1.029, 1.072, 1.116, 1.131 g / cm^3 respectively for pure TBAB: Gly (1: 3) and DES-water complexes in 20:80%, 50:50%; 80:20% and 90:10% v/v. After the addition of water, the distances between the Br^- and the –OH groups from glycerol become longer. This indicates that the hydrogen bonds between the HBA and HBD become weaker, which the theoretical and experimental FT-IR and Raman spectroscopy results confirm [11]. The detailed O–H···Br distances are presented in Table 2.

Table 2 Distances between the Br atom and the –OH group from glycerol components [Å]. The (1), (2), and (3) represent the number of the glycerol molecule that is involved in the hydrogen bond formation with HBD.

Complex	(1) O–H···Br	(2) O–H···Br	(3) O–H···Br
TBAB:Gly (1:3)	2.27	2.47	2.29
80% TBAB:Gly (1:3)–20% H_2O	2.37	2.42	2.38
50% TBAB:Gly (1:3)–50% H_2O	3.20	2.60	2.60
20% TBAB:Gly (1:3)–80% H_2O	3.26	2.62	2.68
10% TBAB:Gly (1:3)–90% H_2O	3.26	2.62	2.79

On the other hand, new strong hydrogen bonds with distances below than 2.5 Å between the –OH groups from water and glycerol (O–H···O–H) and water and water (O–H···O–H), as well as weaker bonds between the Br atom and the hydroxyl groups from water (O–H···Br) with distances higher than 2.55 Å appeared. A graphical presentation of the optimized structures of DES-water complexes with distances between functional groups and reduced density gradient isosurfaces are presented in Figures 6 and 7.

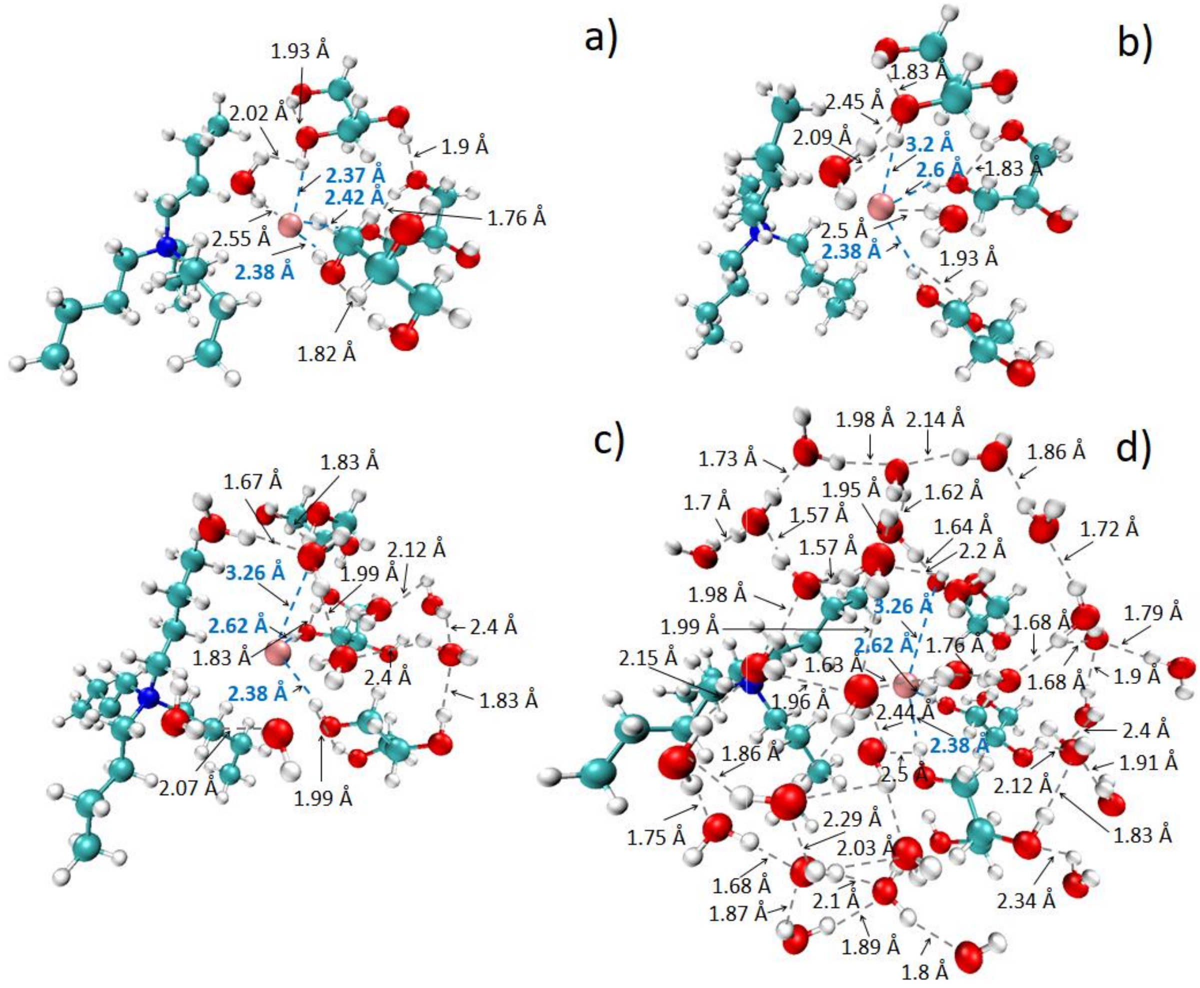

Figure 6 Optimized structures of a) 80% TBAB:Gly (1:3)–20% H_2O; b) 50% TBAB:Gly (1:3)–50% H_2O; c) 20% TBAB:Gly (1:3)–80% H_2O; d) 10% TBAB:Gly (1:3)–90% H_2O

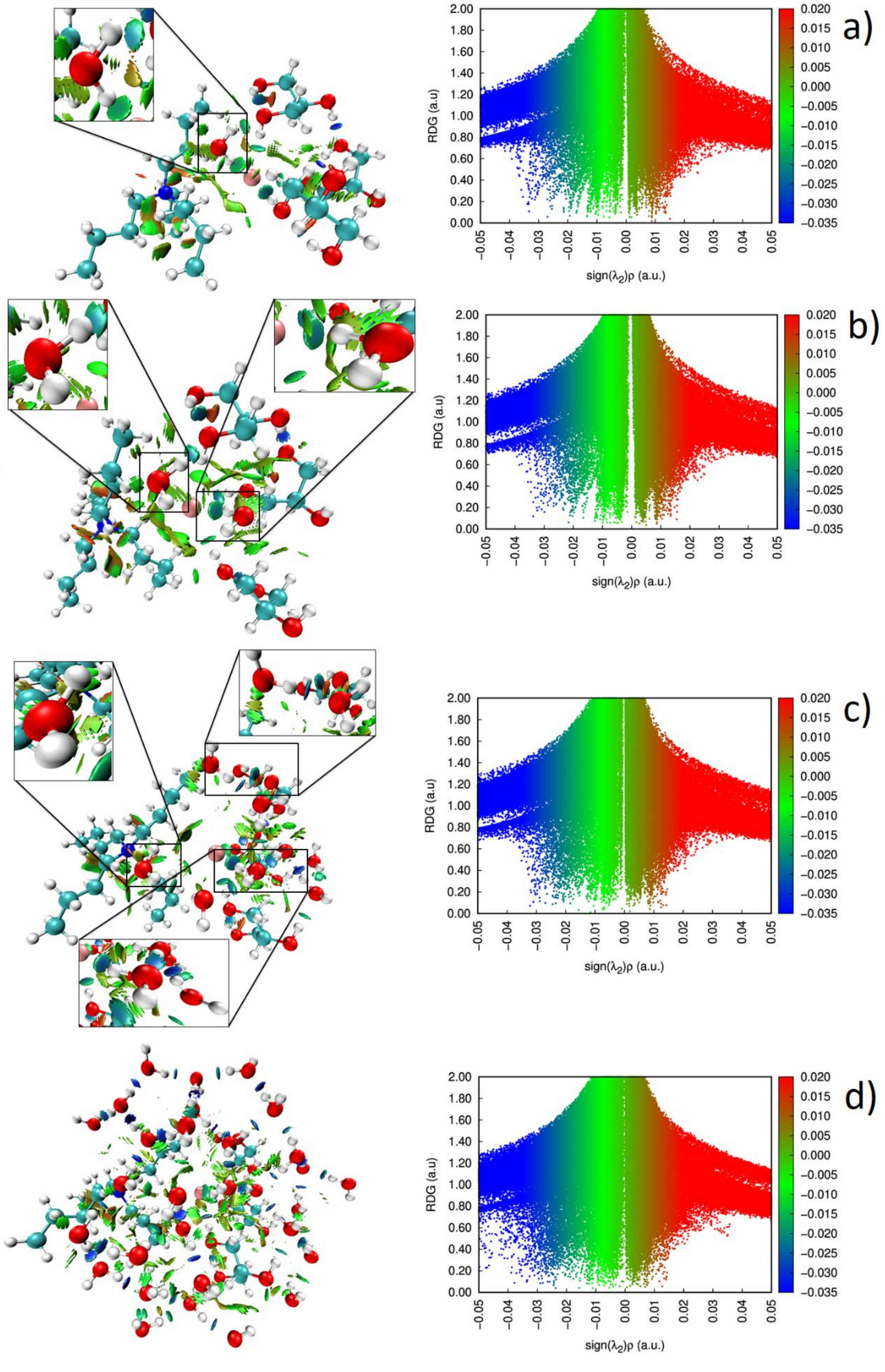

Figure 7 Reduced density gradient isosurfaces (s = 0.5 a.u.) and 2D diagrams of electron density and its reduced density gradient for a) 80% TBAB:Gly (1:3)–20% H_2O; b) 50% TBAB:Gly (1:3)–50% H_2O; c) 20% TBAB:Gly (1:3)–80% H_2O; d) 10% TBAB:Gly (1:3)–90% H_2O

In order to explain of the influence of water addition on the intermolecular interactions of large DES complexes, the center of mass Radial distribution functions (RDF) were studied. The snapshots of TBAB:Gly (1:3)–water complexes are presented in the Figure 8.

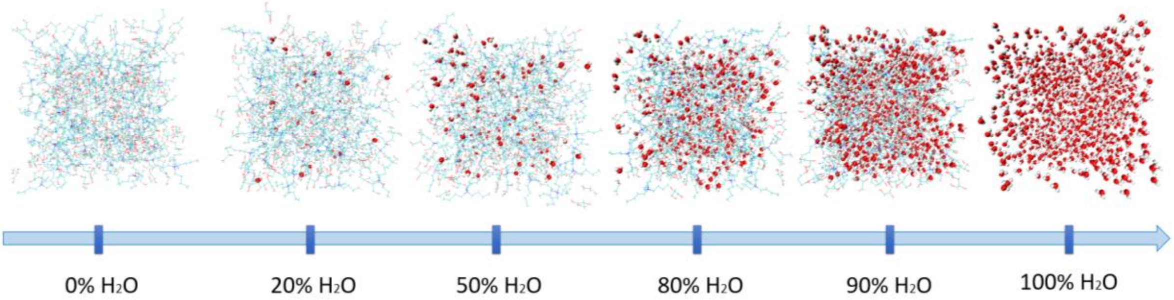

Figure 8 Snapshots of TBAB:Gly (1:3)–water mixtures represents various amount of water.

The results presented in Figure 9 indicate that TBA$^+$–TBA$^+$, TBA$^+$–Br$^-$, Gly–Br$^-$ correlation in large DES-water systems as expected, becomes weaker with the volume of water addition. In all correlations, a decrease in the intensity of the first peak can be observed. However, only in TBA$^+$–TBA$^+$ correlation shifts of the first solvation peak towards a longer length are observed. In the rest of correlation, the position of peaks doesn't not change its position. This indicates a lower effect of the water addition on TBA$^+$–Br$^-$, and Gly–Br$^-$ compared to TBA$^+$–TBA$^+$ pairs. In turn, with the addition of water, an increase in peak intensity and its shift towards lower distances in Gly–Gly and Br$^-$–Br$^-$ correlations can be observed. This indicates that Gly molecules and bromide atoms, come closer in the presence of water in comparison to pure DES. This is probably due to the fact that water even at low concentration is a strong ligand for bromide binding and out-competing DES species due to its hydrogen bonding capability, as well as small molecular volume. Water molecules occupy the space around bromine atoms, which provide to reduce Br$^-$–Br$^-$ separation via bridging in solvent-separated pairs [20]. Similar results were also observed in other works dedicated to DES-H_2O complexes composed of choline chloride:glycolic acid [20], and choline chloride:urea [19,20,35] which proved that the addition of a small amount of water (5-10%) can stabilize the DES network.

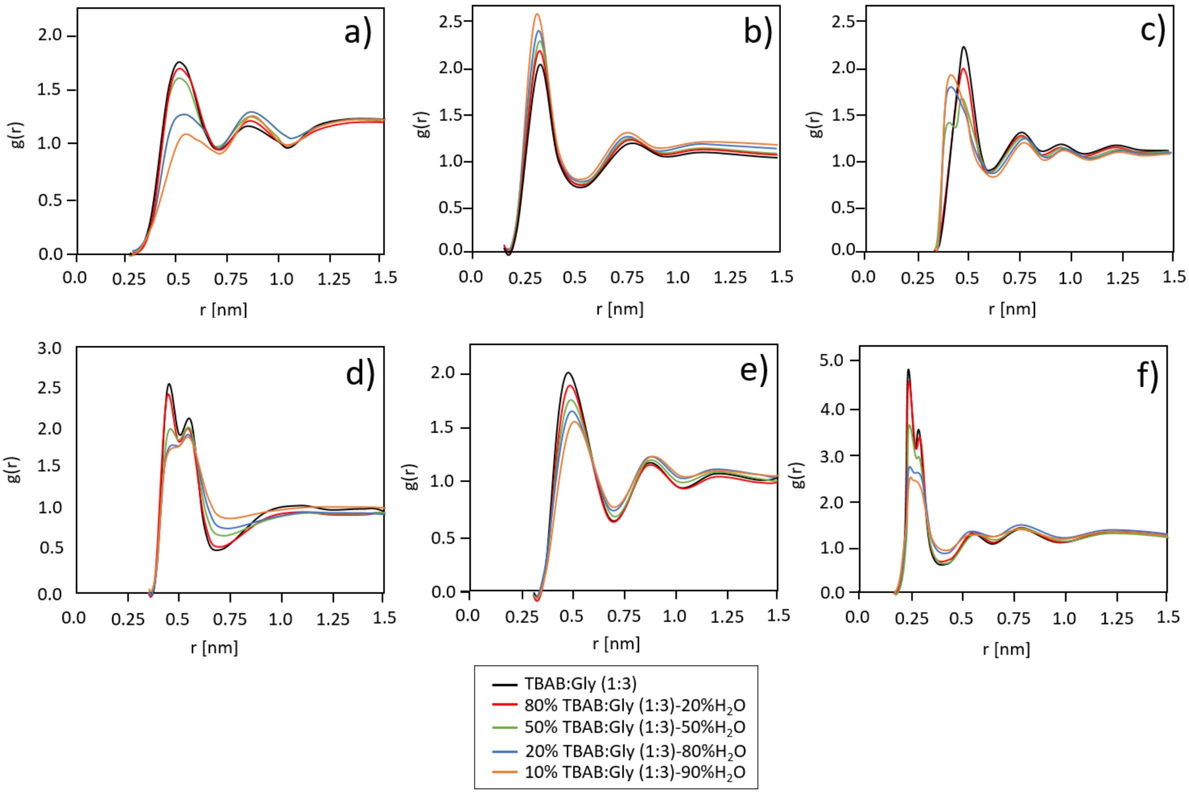

Figure 9 Intermolecular canter of mass Radial distribution functions (RDF) for a) TBA^+–TBA^+; b) Gly–Gly; c) Br^-–Br^-; d) TBA^+–Br^-; e) TBA^+–Gly; f) Br^-–Gly in DES-water systems.

In the next part of the studies, atomic RDF was used to explain how the addition of water affects the hydrogen bonding in DES structures in large systems (Figure 10). The obtained results indicate the decreasing propensity of Br^- atom to the formation of H-bonding with the hydroxyl group from Gly with increasing water volume in DES-H_2O systems. The first solvation peak shifts towards the higher values from about 0.23 to 0.26 mm after the addition of 50% (v/v). Based on the shifts, it can be concluded that typical $Br\cdots HO_{(Gly)}$ hydrogen bonds are destroyed with the addition of minimum 50% (v/v) of water. A further increase in the volume of water causes a further extension of the distance between the Br atom and the hydroxyl groups of Gly (Figure 10). This is probably due to the fact that the water molecules are strong hydrogen-bond donors which provide for enhanced involvement of Br^- water interactions. The similar results were obtained for another atom pair i.e. $N_{(TBAB)}$–Br^-. On the other hand, the first solvation peak shifts towards the lower distance values in $HO_{(Gly)}\cdots HO_{(Gly)}$, after water addition can be observed, which is in line with the above considerations. The similar results was observed for the complex of water and DES composed of choline chloride and ethylene glycol [19].

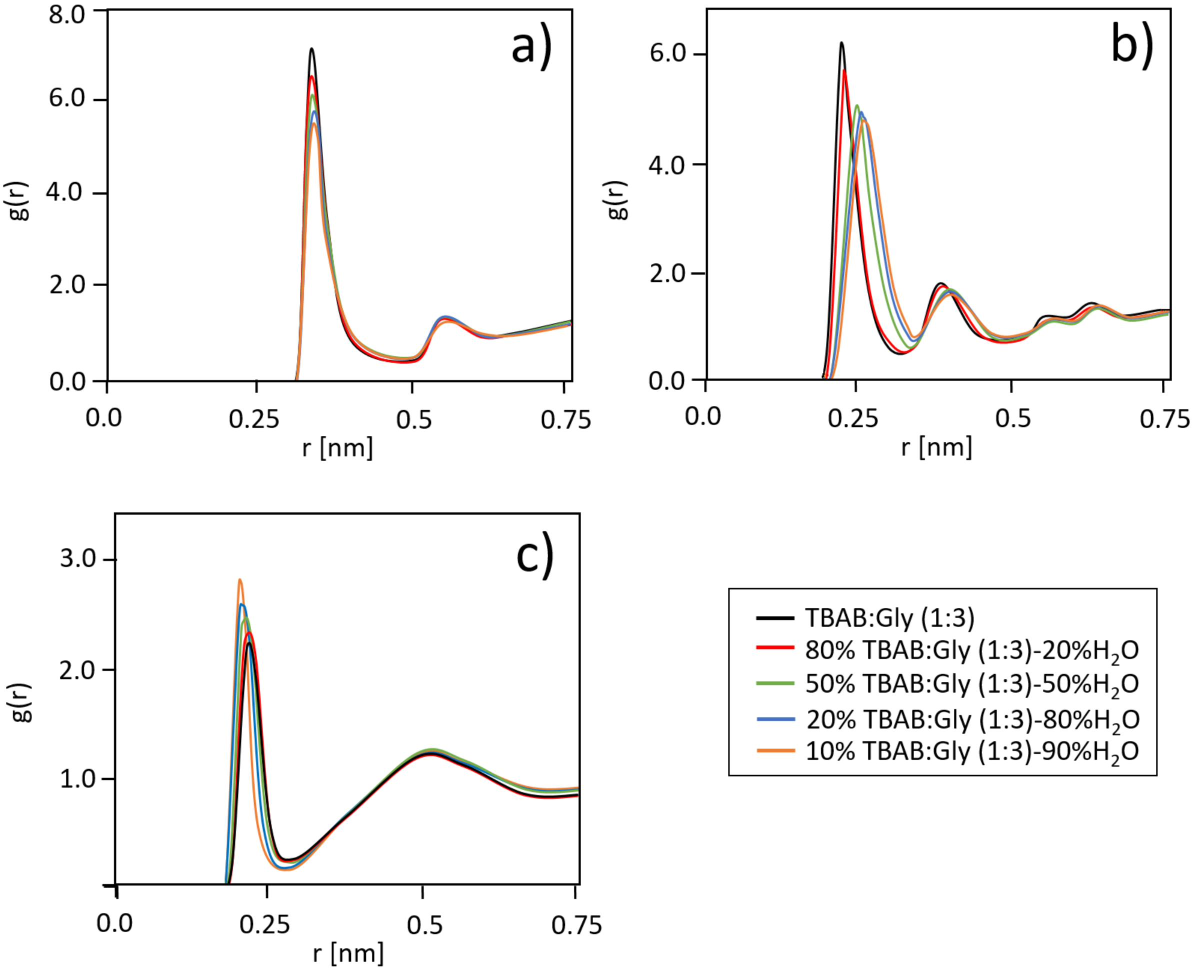

Figure 10 Atomic Radial distribution functions (RDF) for a) $N_{(TBAB)}$–Br^-; b) $OH_{(Gly)}$–Br^-; c) $OH_{(Gly)}$–$HO_{(Gly)}$.

The interaction energy between the HBA and HBD, as well as between the DES and water molecules in most cases is negative, and the lower values indicate stronger interactions inside the complex. The list of calculated interaction energies is presented in Table 3. The calculated values of the DES complexes followed a similar trend as the experimental data: TBAB:Gly (1:3) ~ TBAB:Gly (1:4) < TBAB:Gly (1:2). Despite the weakening of the hydrogen bonds between the HBA and HBD after the addition of water, stronger interaction energies occurred in 10% TBAB:Gly (1:3)–90% H_2O. This is caused by numerous water molecules and the formation of large amounts of hydrogen bonds between them. Along with reduction of the water content in the complexes, the strength of the interaction energy decreases.

Table 3 Interaction energies between HBA and HBD as well as between DES and water

Complex	Interaction energy [kcal/mol]
TBAB:Gly (1:2)	−9.6
TBAB:Gly (1:3)	−11.2
TBAB:Gly (1:4)	−11.0
80% TBAB:Gly (1:3)–20% H_2O	−12.1
50% TBAB:Gly (1:3)–50% H_2O	−16.2
20% TBAB:Gly (1:3)–80% H_2O	−18.1
10% TBAB:Gly (1:3)–90% H_2O	−19.5

4. Conclusion

In the present paper, the results of experimental ^{1}H NMR, ^{13}C NMR, FT-IR and Raman spectroscopy studies of three deep eutectic solvents composed of TBAB and Gly in 1:2, 1:3 and 1:4 molar ratios published very recently [11] were compared with theoretical studies by means of quantum mechanical calculations. In addition, the influence of the varying amounts of added water on the DES structures was also examined using the same procedures. The specific conclusions are as follows:

- The obtained experimental and calculated NMR, FT-IR and Raman spectroscopy results indicate that the hydrogen bonds between TBAB and Gly exist in all the DESs [11]. However, it was difficult to detect how many and where the hydrogen bonds occur. Identification of the number and location of the H-bonds was possible using quantum mechanics calculations. The results of the QM calculations indicate that three type of H-bonds exist in the DES structures, including O–H···Br between Br and Gly, intermolecular O–H···H–O in the Gly structure, and O–H···H–O between the Gly molecules.
- All three types of H-bonds can influence the DES. The number of hydrogen bonds depends on the number of Gly molecules used in the synthesis of the DES. The total number of H-bonds were 5, 7 and 7, in TBAB:Gly (1:2), TBAB:Gly (1:3) and TBAB:Gly (1:4), respectively. This indicates that an increase in Gly molecules (over three Gly molecules) in the DES structures does not increase the number of hydrogen bonds. On the other hand, the complete liquid state of TBAB:Gly (1:4) in comparison to the other DESs indicates that not only H-bonds but also weaker non-bonded interactions, i.e. van der Waals, play an important role in the eutectic mixture formation.
- The small addition of water provides the formation of stable complex TBAB:Gly (1:3)–water. However, a further increase in water content (higher than 50% v/v) provide to the destruction of the most important hydrogen bonds (O–H···Br) in DES structure.

Acknowledgements

V.A. and R.Ch. would like to express their thanks to the Scientific Grant Agency of the Ministry of Education, Science, Research and Sport of the Slovak Republic (VEGA 1/0220/21).

References

[1] A.P. Abbott, D. Boothby, G. Capper, D.L. Davies, R.K. Rasheed, Deep Eutectic Solvents formed between choline chloride and carboxylic acids: Versatile alternatives to ionic liquids, J. Am. Chem. Soc. 126 (2004) 9142–9147. https://doi.org/10.1021/ja048266j.

[2] D. Deng, G. Han, Y. Jiang, Investigation of a deep eutectic solvent formed by levulinic acid with quaternary ammonium salt as an efficient SO2 absorbent, New J. Chem. 39 (2015) 8158–8164. https://doi.org/10.1039/c5nj01629k.

[3] G. Li, Y. Jiang, X. Liu, D. Deng, New levulinic acid-based deep eutectic solvents: Synthesis and physicochemical property determination, J. Mol. Liq. 222 (2016) 201–207. https://doi.org/10.1016/j.molliq.2016.07.039.

[4] H. Wu, M. Shen, X. Chen, G. Yu, A.A. Abdeltawab, S.M. Yakout, New absorbents for hydrogen sulfide: Deep eutectic solvents of tetrabutylammonium bromide/carboxylic acids and choline chloride/carboxylic acids, Sep. Purif. Technol. 224 (2019) 281–289. https://doi.org/10.1016/J.SEPPUR.2019.04.082.

[5] H.F. Hizaddin, M. Sarwono, M. Ali Hashim, I.M. Alnashef, M.K. Hadj-Kali, Coupling the capabilities of different complexing agents into deep eutectic solvents to enhance the separation of aromatics from aliphatics, J. Chem. Thermodyn. 84 (2015) 67–75. https://doi.org/10.1016/j.jct.2014.12.024.

[6] N. Li, Y. Wang, K. Xu, Q. Wen, X. Ding, H. Zhang, Q. Yang, High-performance of deep eutectic solvent based aqueous bi-phasic systems for the extraction of DNA, RSC Adv. 6 (2016) 84406–84414. https://doi.org/10.1039/c6ra17689e.

[7] R. Yusof, E. Abdulmalek, K. Sirat, M.B.A. Rahman, Tetrabutylammonium bromide (TBABr)-Based deep eutectic solvents (DESs) and their physical properties, Molecules. 19 (2014) 8011–8026. https://doi.org/10.3390/molecules19068011.

[8] M.K. Alomar, M. Hayyan, M.A. Alsaadi, S. Akib, A. Hayyan, M.A. Hashim, Glycerol-based deep eutectic solvents: Physical properties, J. Mol. Liq. 215 (2016) 98–103. https://doi.org/10.1016/j.molliq.2015.11.032.

[9] F. Gabriele, M. Chiarini, R. Germani, M. Tiecco, N. Spreti, Effect of water addition on choline chloride/glycol deep eutectic solvents: Characterization of their structural and physicochemical properties, J. Mol. Liq. 291 (2019) 111301. https://doi.org/10.1016/j.molliq.2019.111301.

[10] P. Makoś, G. Boczkaj, Deep eutectic solvents based highly efficient extractive desulfurization of fuels – Eco-friendly approach, J. Mol. Liq. 296 (2019) 111916–111927. https://doi.org/10.1016/j.molliq.2019.111916.

[11] R. Chromá, M. Vilková, I. Shepa, P. Makoś-Chełstowska, V. Andruch, Investigation of tetrabutylammonium bromide-glycerol-based deep eutectic solvents and their mixtures with water by spectroscopic techniques, J. Mol. Liq. 330 (2021) 115617. https://doi.org/10.1016/j.molliq.2021.115617.

[12] T. Aissaoui, Y. Benguerba, M.K. AlOmar, I.M. AlNashef, Computational investigation of the microstructural characteristics and physical properties of glycerol-based deep eutectic solvents, J. Mol. Model. 23 (2017). https://doi.org/10.1007/s00894-017-3450-5.

[13] M. Mohan, P.K. Naik, T. Banerjee, V. V. Goud, S. Paul, Solubility of glucose in tetrabutylammonium bromide based deep eutectic solvents: Experimental and molecular dynamic simulations, Fluid Phase Equilib. 448 (2017) 168–177. https://doi.org/10.1016/j.fluid.2017.05.024.

[14] P.K. Naik, S. Paul, T. Banerjee, Physiochemical Properties and Molecular Dynamics Simulations of Phosphonium and Ammonium Based Deep Eutectic Solvents, J. Solution Chem. 48 (2019) 1046–1065. https://doi.org/10.1007/s10953-019-00903-0.

[15] M. Saha, M. Saha, M.S. Rahman, M.N. Hossain, D.E. Raynie, M.A. Halim, Molecular and Spectroscopic Insights of a Choline Chloride Based Therapeutic Deep Eutectic Solvent, J. Phys. Chem. A. 124 (2020) 4690–4699. https://doi.org/10.1021/acs.jpca.0c00851.

[16] E. Słupek, P. Makoś, Absorptive Desulfurization of Model Biogas Stream Using Choline Chloride-Based Deep Eutectic Solvents, Sustainability. 12 (2020) 1619–1635.

https://doi.org/10.3390/su12041619.

[17] P. Makoś, E. Słupek, J. Gębicki, Extractive detoxification of feedstocks for the production of biofuels using new hydrophobic deep eutectic solvents – Experimental and theoretical studies, J. Mol. Liq. (2020) in press. https://doi.org/10.1016/j.molliq.2020.113101.

[18] P. Makoś, A. Przyjazny, G. Boczkaj, Hydrophobic deep eutectic solvents as “green” extraction media for polycyclic aromatic hydrocarbons in aqueous samples, J. Chromatogr. A. 1570 (2018). https://doi.org/10.1016/j.chroma.2018.07.070.

[19] S. Kaur, A. Gupta, H.K. Kashyap, H.K. Kashyap, How Hydration Affects the Microscopic Structural Morphology in a Deep Eutectic Solvent, J. Phys. Chem. B. 124 (2020) 2230–2237. https://doi.org/10.1021/acs.jpcb.9b11753.

[20] M.E. Di Pietro, O. Hammond, A. Van Den Bruinhorst, A. Mannu, A. Padua, A. Mele, M. Costa Gomes, Connecting chloride solvation with hydration in deep eutectic systems, Phys. Chem. Chem. Phys. 23 (2021) 107–111. https://doi.org/10.1039/d0cp05843b.

[21] S. Zhu, H. Li, W. Zhu, W. Jiang, C. Wang, P. Wu, Q. Zhang, H. Li, Vibrational analysis and formation mechanism of typical deep eutectic solvents: An experimental and theoretical study, J. Mol. Graph. Model. 68 (2016) 158–175. https://doi.org/https://doi.org/10.1016/j.jmgm.2016.05.003.

[22] V. Krishnakumar, V. Balachandran, T. Chithambarathanu, Density functional theory study of the FT-IR spectra of phthalimide and N-bromophthalimide, Spectrochim. Acta - Part A Mol. Biomol. Spectrosc. 62 (2005) 918–925. https://doi.org/10.1016/j.saa.2005.02.051.

[23] S. Simon, M. Duran, J.J. Dannenberg, How does basis set superposition error change the potential surfaces for hydrogen-bonded dimers?, J. Chem. Phys. 105 (1996) 11024–11031. https://doi.org/10.1063/1.472902.

[24] T. Lu, F. Chen, Multiwfn: A multifunctional wavefunction analyzer, J. Comput. Chem. 33 (2012) 580–592. https://doi.org/10.1002/jcc.22885.

[25] T. Lu, F. Chen, Quantitative analysis of molecular surface based on improved Marching Tetrahedra algorithm, J. Mol. Graph. Model. 38 (2012) 314–323. https://doi.org/10.1016/j.jmgm.2012.07.004.

[26] E.R. Johnson, S. Keinan, P. Mori-Sánchez, J. Contreras-García, A.J. Cohen, W. Yang, Revealing noncovalent interactions, J. Am. Chem. Soc. 132 (2010) 6498–6506. https://doi.org/10.1021/ja100936w.

[27] J.M. Martínez, L. Martínez, Packing optimization for automated generation of complex system’s initial configurations for molecular dynamics and docking, J. Comput. Chem. 24 (2003) 819–825. https://doi.org/10.1002/jcc.10216.

[28] M. Parrinello, A. Rahman, Polymorphic transitions in single crystals: A new molecular dynamics method, J. Appl. Phys. 52 (1981) 7182–7190. https://doi.org/10.1063/1.328693.

[29] S. Nosé, A unified formulation of the constant temperature molecular dynamics methods, J. Chem. Phys. 81 (1984) 511–519. https://doi.org/10.1063/1.447334.

[30] S. Nosé, S. Nosi~, Molecular Physics: An International Journal at the Interface Between Chemistry and Physics A molecular dynamics method for simulations in the canonical ensemble A molecular dynamics method for simulations in the canonical ensemblet, An Int. J.

Interface Between Chem. Phys. Mol. Phys. 52 (1984) 255–268.

[31] H.J.C. Berendsen, J.R. Grigera, T.P. Straatsma, The missing term in effective pair potentials, J. Phys. Chem. 91 (1987) 6269–6271. https://doi.org/10.1021/j100308a038.

[32] B. Hess, C. Kutzner, D. Van Der Spoel, E. Lindahl, GRGMACS 4: Algorithms for highly efficient, load-balanced, and scalable molecular simulation, J. Chem. Theory Comput. 4 (2008) 435–447. https://doi.org/10.1021/ct700301q.

[33] D. Van Der Spoel, E. Lindahl, B. Hess, G. Groenhof, A.E. Mark, H.J.C. Berendsen, GROMACS: Fast, flexible, and free, J. Comput. Chem. 26 (2005) 1701–1718. https://doi.org/10.1002/jcc.20291.

[34] H. Sasaki, S. Daicho, Y. Yamada, Y. Nibu, Comparable strength of OH-O versus OH-π hydrogen bonds in hydrogen-bonded 2,3-benzofuran clusters with water and methanol, J. Phys. Chem. A. 117 (2013) 3183–3189. https://doi.org/10.1021/jp400676x.

[35] P. Kumari, Shobhna, S. Kaur, H.K. Kashyap, Influence of Hydration on the Structure of Reline Deep Eutectic Solvent: A Molecular Dynamics Study, ACS Omega. 3 (2018) 15246–15255. https://doi.org/10.1021/acsomega.8b02447.